# Scaling with temperature and concentration of the nonlinear rheology of a soft hexagonal phase

Laurence Ramos
*Groupe de Dynamique des Phases Condensées (UMR CNRS-UM2 5581), CC26, Université Montpellier 2, 34095 Montpellier Cedex 5, France*

(Received 18 May 2001; published 19 November 2001)

The nonlinear rheology of a soft surfactant hexagonal phase is examined. The system exhibits a shear-melting transition from a two-dimensional polycrystalline texture to a liquid of cylinders aligned along the flow [Ramos *et al.*, Langmuir **16**, 5846 (2000)]. This dynamic transition is associated with a discontinuity in the stress-strain curve (flow curve). A detailed study of the temperature and concentration dependence of the flow curves is presented. The nonlinear rheology is found to display a scaling behavior, when temperature or concentration are varied. We demonstrate that the whole behavior of the hexagonal phase under shear is essentially governed by the linear shear modulus of the sample, $G_0$. When temperature is varied, we show that the two key parameters, which control $G_0$ and in turn, the flow curve, are a transition temperature $T_c$ and an activation energy $E_A$. We propose $E_A$ to be related to the scission energy of one cylinder into two pieces.

DOI: 10.1103/PhysRevE.64.061502 PACS number(s): 83.50.−v, 82.70.−y, 62.20.Dc, 61.30.−v

## I. INTRODUCTION

The behavior of complex fluids under shear has been extensively studied using rheology. Very often, the coupling between the structure and the flow field induces dynamic transitions [1,2]. These transitions are either phase transitions, which can also occur at rest, or textural transitions, which solely occur under shear. In both cases, one signature of such a transition is a discontinuity in the flow curve (stress vs shear rate plot) of the sample. Concerning liquid crystalline or crystalline samples, extensive experiments have been devoted to soft three-dimensional (3D) crystals [3–6] and to lamellar phases [7–10]. The latter system, a 1D solid and 2D liquid, has turned out to display rich and fascinating behaviors under shear.

Very few studies exist, however, on the ''dual'' system, a 1D liquid and 2D solid, that is, the hexagonal or columnar phase [11–13]. Using melts of block copolymers Morrison *et al.* [11] have provided one of the few examples of shear-induced morphological transitions on hexagonal phases. At high rates, the authors show the coexistence of two types of grains of hexagonal phase, but whose nature has not been clearly identified. Using lyotropic hexagonal phases of surfactant [14], we have been able for the first time to unambiguously correlate a discontinuity in the flow curve with a structural transition in a hexagonal liquid crystalline system [15]. The shear-induced transition is a melting of the long-range 2D order of the cylinders, resulting in a liquid of infinite cylinders strongly aligned along the flow. The physical mechanisms at the origin of the shear melting remain at present unclear but some understanding may certainly be gained by a detailed investigation of the flow curves.

In this paper, we report a careful study of the flow curves of soft hexagonal phases, varying independently two control parameters, the temperature and the concentration. The nonlinear rheology exhibits a scaling behavior as temperature or concentration are varied. We show that the shear modulus of the hexagonal phase, $G_0$, controls the whole behavior of the system under shear. The nonlinear rheology of a hexagonal appears, therefore, solely controlled by its linear elasticity. In particular, we demonstrate that only two quantities, an activation energy $E_A$ and a transition temperature $T_c$, are sufficient to capture the temperature dependence of $G_0$ and, in turn, the main features of the behavior of the system under shear. Both the low shear regime and the high shear regime, where the long-range 2D order is melted, are governed by the same activation energy $E_A$, which is proposed to be related to the scission energy, the energetic cost to break a cylinder into two pieces.

The paper is organized as follows. The experimental system is described in Sec. II and the dependence of the flow curves on temperature and concentration is presented in Sec. III. The results are discussed in Sec. IV; the crucial role of the linear shear modulus is evidenced in Sec. IV A, and the physical meanings of the transition temperature and the activation energy are commented in Sec. IV B.

## II. EXPERIMENTAL SYSTEM

We used lyotropic hexagonal phases of direct type [16], which consist of infinite oil cylinders, coated with a surfactant monolayer and arranged on a triangular lattice in an aqueous medium. They comprise a mixture of sodium dodecylsulfate as surfactant, pentanol as cosurfactant, salted water (NaCl), and cyclohexane as oil. By varying concomitantly the oil content and the ionic strength of the polar medium, the radius $R$ of the oil-swollen cylinders can be varied over 1 decade, from 1.5 nm (without oil) to 17 nm, while the distance $h$ between the cylinders walls is kept small and constant ($h \cong 2.5$ nm) [14]. We define the swelling ratio $\rho$ as the ratio of the volume of oil to the volume of water, $\rho = V_{\text{oil}}/V_{\text{water}}$, which can be continuously varied from 0 up to 3.8.

Two parameters are varied in this work, namely, the temperature and the concentration of oil cylinders, i.e., the swelling ratio. In a first set of experiments, we investigate a swollen phase with $\rho = 3.24$ (corresponding to $R = 15$ nm) at different temperatures, ranging from 12 °C up to 36 °C. Small-angle x-ray scattering (SAXS) experiments on this system [17] have shown that, in the range 14–40 °C, the

 

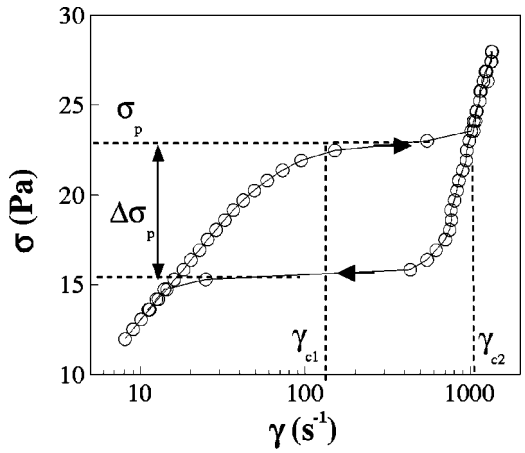


FIG. 1. Flow curve, shear stress $\sigma$ as a function of shear rate $\gamma$, of a swollen hexagonal phase ($\rho=3.24$), showing the different parameters characterizing the dynamic transition $\sigma_p$, $\Delta\sigma_p$, $\gamma_{c1}$ and $\gamma_{c2}$. The arrows give the direction of the measurements. Temperature is 20 °C.

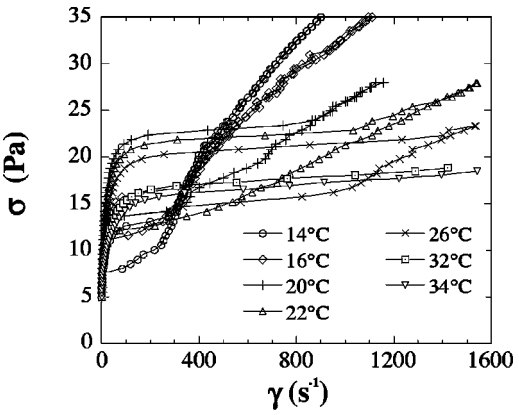


FIG. 2. Flow curves, shear stress $\sigma$ as a function of shear rate $\gamma$, of a swollen hexagonal phase ($\rho=3.24$). Data sets are labeled by temperature. For the sake of clarity, all experimental curves are not represented.

hexagonal phase is stable and that the lattice parameter does not vary; moreover, at 12 °C, a phase transition from the hexagonal phase to a liquid isotropic phase occurs.

In a second set of experiments, we vary the swelling ratio of the hexagonal phase at a fixed temperature of 20 °C, and study swollen systems with $\rho$ ranging from 2.9 up to 3.8, corresponding to radius $R$ from 13 nm up to 17 nm.

## III. SCALING BEHAVIOR OF THE FLOW CURVES

Rheology experiments are performed in a Couette geometry with a stress-controlled Paar Physica UDS 200 rheometer. The flow curve, stress $\sigma$ vs shear rate $\gamma$, of a swollen hexagonal phase, obtained imposing either $\sigma$ or $\gamma$, has been described in detail in Ref. [15]. In this paper, we focus on the curves obtained by imposing the stress. A typical flow curve is shown in Fig. 1. At low shear rates, the system is shear thinning, while at high rates, the stress varies linearly with the shear rate. These two extreme regimes correspond to two stable branches of stationary states, thereafter, referred to as lower and higher branches, respectively. The passage from the lower branch to the higher branch occurs through a marked drop of viscosity. (By analogy with Newtonian fluids, an effective viscosity $\eta$ is defined through $\sigma=\eta\gamma$.) The drop of viscosity corresponds to a plateaulike variation of the stress, in the $\sigma$ vs $\gamma$ plot (Fig. 1). A high plateau is obtained when increasing the stress and a lower one is obtained upon decreasing $\sigma$. The flow curve defines, therefore, a perfectly reproducible hysteretic loop. The hysteresis is the signature of a bistable system for which the shear rate is a multivalued function of the shear stress, as has already been observed for lamellar phases under shear [9,18]. We call $\sigma_p$ the high plateau value, and $\Delta\sigma_p$ the difference between the high and low plateaus, that is, the width of the hysteresis (Fig. 1). The critical shear rates for the starts and finishes off the high plateau are called $\gamma_{c1}$ and $\gamma_{c2}$, respectively.

The structure of the hexagonal phase in the two stable branches has been previously characterized using SAXS under shear [15]. The main scattering results can be summarized as follows. At low shear, on the lower branch, the hexagonal phase exhibits a polycrystalline structure with the cylinders preferentially oriented along the velocity direction. The grains of the polycrystal are progressively aligned with increasing shear rate. At high shear rate, on the higher branch, the long-range 2D order of the cylinders has melted, leading to a 2D liquid of cylinders strongly aligned along the flow.

### A. Scaling with temperature

#### *1. Shear-melting transition*

The flow curves obtained at different temperatures, from 14 °C to 36 °C, are presented in Fig. 2. In the range of temperatures investigated, all curves are qualitatively similar: they display two stable branches, separated by plateaulike variations of the stress, with the presence of a hysteresis. However, the quantitative parameters that characterize the flow curves vary strongly. These marked changes may *a priori* seem surprising, since in this range of temperature, the hexagonal phase keeps the same structure with a constant lattice parameter.

We start the quantitative analysis by the higher branch. In this regime, the stress varies linearly with the shear rate. For each temperature $T$, one can thus determine the effective viscosity $\eta$ of the melted phase. The values of $\eta$ are reported in Fig. 3 and show a decrease of the viscosity from 30 cP down to 14 cP when $T$ increases from 14 °C to 22 °C. (No data can be obtained above 22 °C because the shear rate at which the higher branch should start is larger than the upper limit of our rheometer.) The viscosity decrease can be accounted for by an Arrhenius form, $\eta=\eta_0\exp(E_A/kT)$, with an activation energy $E_A$ of 30 $kT$ (inset of Fig. 3).

Concerning the critical shear rates, we focus here on $\gamma_{c2}$ because the experimental determination of $\gamma_{c1}$ is more delicate. Data are displayed in Fig. 4 and show a monotonous increase of the critical shear rate $\gamma_{c2}$ with temperature, from 300 to 1400 $s^{-1}$, for $T$ between 14 °C and 22 °C. Quantitatively, we find that $\gamma_{c2}$ is proportional to $(T-T_c)$, with a

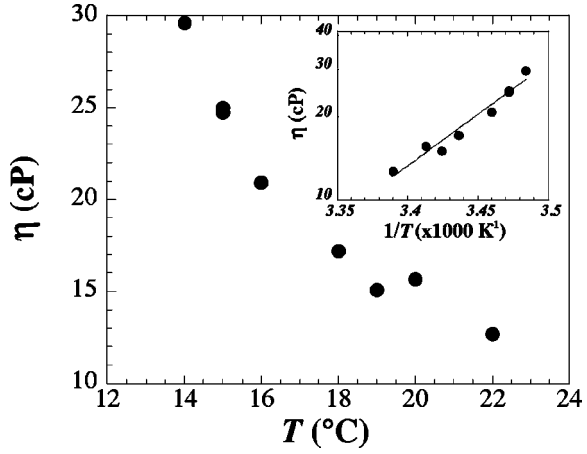


FIG. 3. Temperature dependence of the viscosity in the higher branch for a sample with $\rho = 3.24$. Inset: same data as in the main plot represented in an Arrhenius plot ($\ln \eta$ as a function of $1/T$). The solid line is an Arrhenius fit yielding an activation energy $E_A = 30\ kT$.

transition temperature $T_c = 12\,^{\circ}\mathrm{C}$.

Contrary to the critical shear rate, the stress plateau $\sigma_p$ varies in a nonmonotonous way with temperature. As can be seen in the inset of Fig. 4, the stress plateau is maximal for $T = 20\,^{\circ}\mathrm{C}$; $\sigma_p$ increases from 13 to 23.2 Pa, when $T$ increases from $14\,^{\circ}\mathrm{C}$ to $20\,^{\circ}\mathrm{C}$, and then decreases down to 16 Pa, when $T$ reaches $36\,^{\circ}\mathrm{C}$. A qualitatively analogous variation is obtained for the width of the hysteresis $\Delta\sigma_p$. To gain insight into the nonmonotonous temperature dependence of the stress quantities $\sigma_p$ and $\Delta\sigma_p$, let us normalize, in a first step, $\sigma$ by the activation term found above in the high shear regime. We, therefore, define a normalized stress as

$$\tilde{\sigma} = \sigma \times [\exp(E_A/kT_0)/\exp(E_A/kT)], \tag{1}$$

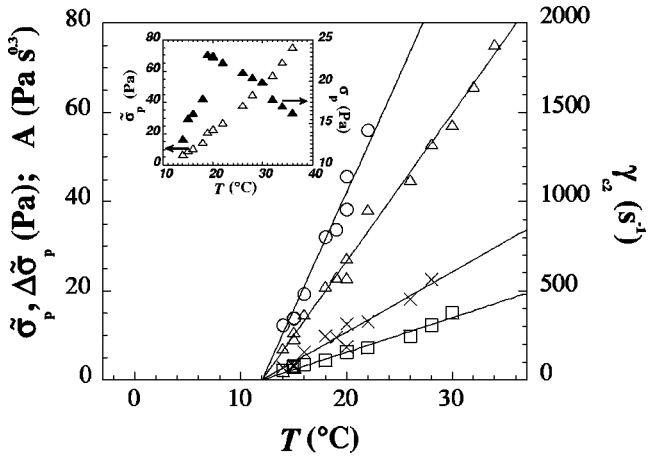


FIG. 4. Temperature dependence of $\tilde{\sigma}_p$ (triangles), $\Delta\tilde{\sigma}_p$ (crosses), $A$ (squares), and critical shear rate $\gamma_{c2}$ (circles) extracted from the data of Fig. 2 (see text for the definition of these quantities). The lines are linear fits of the data points. Inset: raw stress plateau values $\sigma_p$ (solid symbols) and normalized values $\tilde{\sigma}_p$ (empty symbols) as a function of temperature.

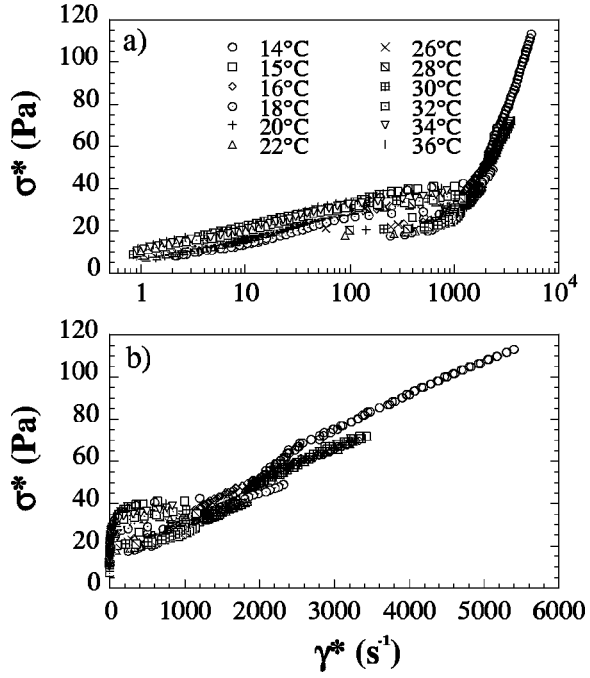


FIG. 5. Same data as in Fig. 2 plotted in the rescaled units (see text), (a) linear-logarithmic representation and (b) linear-linear representations.

where $E_A = 30\,kT$ is the activation energy found in the high shear rate regime and $T_0 = 293$ K. Note that the temperature $T_0 = 293$ K is chosen to allow a direct comparison with the experiments on samples with different swelling ratios always performed at $T_0 = 293$ K. Similarly, one defines

$$\tilde{\sigma}_p = \sigma_p \times [\exp(E_A/kT_0)/\exp(E_A/kT)], \tag{2}$$

$$\Delta\tilde{\sigma}_p = \Delta\sigma_p \times [\exp(E_A/kT_0)/\exp(E_A/kT)]. \tag{3}$$

Surprisingly enough, using such normalization, a monotonous increase of the two quantities $\tilde{\sigma}_p$ and $\Delta\tilde{\sigma}_p$ with temperature $T$ is recovered (Fig. 4). Moreover, Fig. 4 shows that $\tilde{\sigma}_p(T)$ and $\Delta\tilde{\sigma}_p(T)$ have the same temperature dependence as $\gamma_{c2}$:

$$\tilde{\sigma}_p \sim \Delta\tilde{\sigma}_p \sim \gamma_{c2} \sim (T - T_c) \tag{4}$$

with $T_c = 12\,^{\circ}\mathrm{C}$.

Consequently, if we define rescaled units as $\sigma^* = \tilde{\sigma} \times T_c/(T - T_c)$ and $\gamma^* = \gamma \times T_c/(T - T_c)$ and replot all the curves obtained at different temperatures in the $(\sigma^*, \gamma^*)$ plane, a reasonably good collapse of the data is achieved as shown in Fig. 5 and by the relatively well-defined rescaled parameters characterizing the transition independently of temperature: $\gamma^*_{c2} = 1330 \pm 290\ \mathrm{s}^{-1}$, $\sigma^*_p = 35 \pm 5$ Pa, and $\Delta\sigma^*_p = 13 \pm 1$ Pa. Although the master curve obtained with these rescaled units is not perfect, we believe that the scaling captures the essential features for the flow of a hexagonal phase. Moreover, the existence of a universal curve strongly suggests that only two parameters, namely, the activation en-

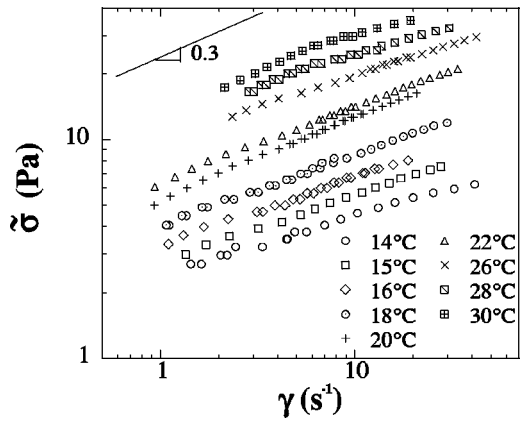


FIG. 6. Normalized stress $\tilde{\sigma}$ as a function of shear rate in the lower branch (low shear). Data sets are labeled by temperature and are parts of the flow curves of Fig. 2.

ergy $E_A$ and the transition temperature $T_c$ are sufficient to account for the dynamic transition and for the behavior under high shear.

#### *2. Low shear rate regime*

In this section, we focus on the low shear rate regime, that is, well below the dynamic transition towards the melted phase. In this regime, the shear stress varies as a power law with the shear rate $\sigma \sim \gamma^m$ (Fig. 6). For the set of temperatures investigated, the exponent $m$ is almost constant. The fitting procedures give an exponent between 0.26 and 0.37. By fitting the data forcing a unique exponent for all temperatures, we determine this exponent to be $m=0.30$. We define then a prefactor $A$, such that, in the lower branch, the following relationship holds:

$$\sigma = A \times [\exp(E_A/kT)/\exp(E_A/kT_0)]\gamma^{0.3} \tag{5}$$

or equivalently

$$\tilde{\sigma} = A \times \gamma^{0.3}. \tag{6}$$

The dependence of $\tilde{\sigma}$ on temperature and shear rate is given in Fig. 6. The values of the prefactor $A$ are extracted from a fit of the data using Eq. (6), and are reported in Fig. 4. Again, we find a scaling with $(T-T_c)$, with a transition temperature equal to that previously obtained ($T_c=12\,^\circ$C).

#### *3. Conclusion*

To conclude, we have shown that both the prefactor $A$ in the shear thinning behavior at low shear rate and the parameters that characterize the dynamic transition, namely, the critical shear rate, $\gamma_{c2}$, and the normalized stress plateau and width of the hysteretic loop, $\tilde{\sigma}_p$ and $\Delta\tilde{\sigma}_p$, respectively, vary similarly with temperature:

$$A \sim \tilde{\sigma}_p \sim \Delta\tilde{\sigma}_p \sim \gamma_{c2} \sim (T-T_c). \tag{7}$$

Thus, the following scaling holds for the stress plateau $\sigma_p$ and the stress width of the hysteresis:

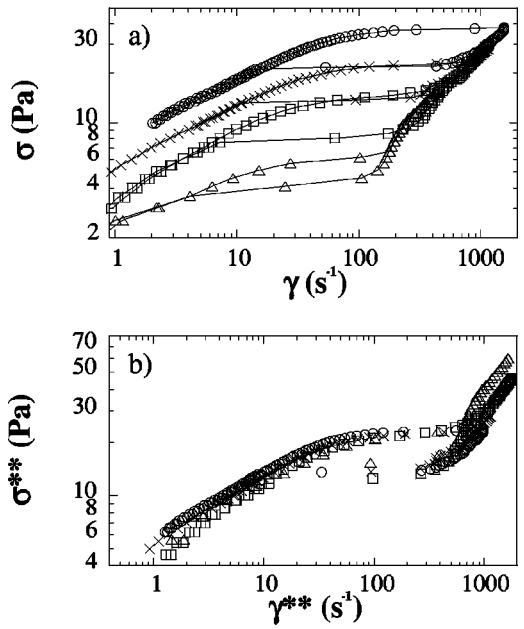


FIG. 7. (a) Flow curves at $T=20\,^\circ$C for samples with different swelling ratios, $\rho=2.86$ (triangles), $\rho=3.24$ (squares), $\rho=3.51$ (crosses), and $\rho=3.77$ (circles). (b) Same data plotted in the rescaled plane ($\gamma^{**},\sigma^{**}$) (see text for the definition of the rescaled units).

$$\sigma_p \sim \Delta\sigma_p \sim [\exp(E_A/kT)] \times (T-T_c). \tag{8}$$

All quantities present a critical-like variation with temperature, with the same transition temperature $T_c=12\,^\circ$C. Our analysis underlines, therefore, the relevance of two parameters, the transition temperature $T_c$ and the activation energy $E_A$. These two parameters are found to control the dynamic transition as well as the shear thinning regime at low shear rate. This implies, in particular, that the same activation energy controls the behavior in the low shear rate regime, where a polycrystalline hexagonal phase flows, and in the high shear rate regimes where the long-range order has melted. This result is commented later on (Sec. IV).

### B. Scaling with the swelling

We measure the flow curves of hexagonal phases with different swelling ratios $\rho$. Experiments are performed at a fixed temperature of 20 °C. The range of swelling ratio accessible is rather limited because of experimental problems at low $\rho$. In fact, for stiff systems (low $\rho$), high shear rates lead to the formation of bubbles in the sample cell that prevent the achievement of reliable results. The swelling ratio is, therefore, varied between 2.86 and 3.77 and the corresponding flow curves are shown in Fig. 7(a). While the global shape of the curves is maintained, the quantitative parameters display marked variations with $\rho$. An increase of $\rho$ of about 30% induces a decrease of the stress plateau $\sigma_p$ and critical shear rate $\gamma_{c2}$ by almost one order of magnitude, from 6 Pa to 36 Pa and 180 $s^{-1}$ to 1560 $s^{-1}$, respectively. Let us normalize both the stress and the shear rate by the high stress plateau value of the flow curves. We define thus:

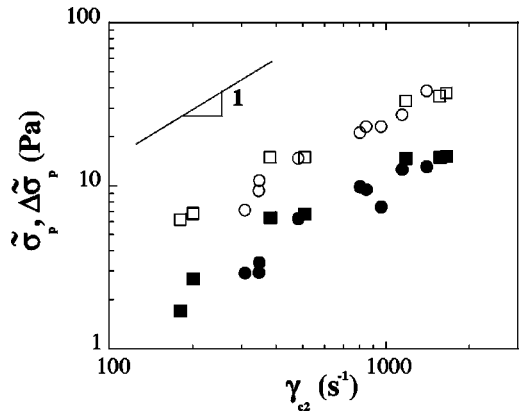


FIG. 8. Normalized high stress plateau values $\tilde{\sigma}_p$ (full symbols) and normalized difference between high and low stress plateaus $\Delta\tilde{\sigma}_p$ (empty symbols) as a function of critical shear rate $\gamma_{c2}$. The squares correspond to data obtained at $T=20°C$ for samples with different swellings $\rho$ while the circles correspond to data obtained at different temperatures for a sample with $\rho=3.24$.

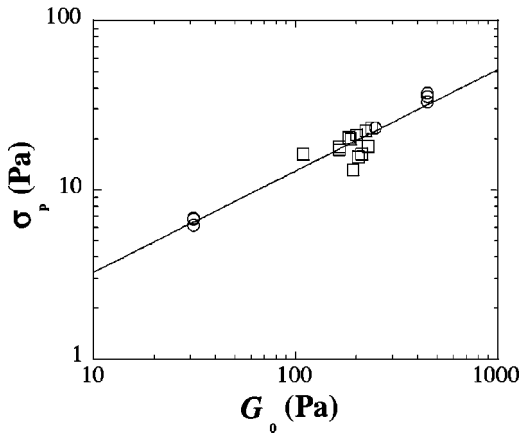


FIG. 9. Stress plateau as a function of the elastic modulus; the circles correspond to results obtained with samples of different swelling ratios $\rho$ at a fixed temperature of 20 °C, while the squares correspond to results obtained at different temperatures for a sample with $\rho=3.24$. The straight line has a slope of 0.6.

$$\sigma^{**}=\sigma\times(\sigma_p^0/\sigma_p), \tag{9}$$

$$\gamma^{**}=\gamma\times(\sigma_p^0/\sigma_p), \tag{10}$$

where $\sigma_p^0$ is the stress plateau for the sample with a swelling ratio of 3.24 ($\sigma_p^0=23.2$ Pa). (This is the sample whose behavior with temperature is investigated in the previous section.) Using these normalized quantities, a reasonably good collapse of all the flow curves onto a single master curve is obtained [Fig. 7(b)] as shown by the determination of the critical parameters characterizing the transition, independently of the swelling: $\gamma_{c2}^{**}=815\pm150$ $s^{-1}$, $\sigma_p^{**}=22.9\pm0.3$ Pa, and $\Delta\sigma_p^{*}=9.2\pm1.1$ Pa. Thus, at a given temperature, one parameter is sufficient to account for the whole behavior, which suggests a universal shape for the flow curves.

## IV. DISCUSSION

In this section, we analyze how the parameters characterizing the shear-melting transition vary and we show that they depend uniquely on the shear modulus of the sample. We then, comment on the transition temperature and on the activation energy, the two parameters that have been found to govern the temperature dependence of the nonlinear rheology.

### A. Role of the linear shear modulus

In the range of swelling and temperature investigated, all the parameters characterizing the shear-melting transition vary in a consistent way. This is shown in the plot of $\tilde{\sigma}_p(T)$ and $\Delta\tilde{\sigma}_p(T)$ as a function of $\gamma_{c2}$ (Fig. 8), which demonstrates that both values obtained at different temperatures and those obtained at different swellings collapse and present a linear variation with the critical shear rate $\gamma_{c2}$ [19]. Note that the linear variation of $\tilde{\sigma}_p(T)$ with $\gamma_{c2}$ simply proves that the higher branch is characterized by a unique viscosity, which does not strongly depend on the swelling ratio but rather varies with temperature following an Arrhenius form. More important, the collapse of data of Fig. 8 enables a unification of the two sets of experiments. It underlines that, in both cases, the same physical parameters control the transition from the aligned polycrystalline phase to the melted phase, and that these parameters can be varied by changing either the temperature or the swelling.

In this context, we demonstrate below the crucial role played by the linear elastic modulus of the system, $G_0$. The variation of the elastic modulus $G_0$ with the swelling ratio, at a fixed temperature of 20 °C, has been previously measured [20]. On the other hand, the temperature dependence of $G_0$ is investigated here, for a sample with a swelling ratio $\rho=3.24$ [21]. We plot in Fig. 9 the two sets of values of the elastic modulus as a function of the stress plateau $\sigma_p$. A collapse of all data, measured at different temperatures and different swelling ratios, is obtained. Thus, Fig. 9 demonstrates a strong correlation between the stress plateau and the shear modulus $G_0$ of the hexagonal phase. Quantitatively, we find that $\sigma_p\sim G_0^{0.6}$ over more than one order of magnitude, even though a slight departure from this scaling is observed for the data obtained at low temperatures [22]. This strongly suggests that the key parameter for the control of the flow curve is, indeed, the elastic modulus $G_0$. Thus, the nonlinear rheology appears uniquely controlled by one linear elastic modulus of the system.

The scaling found above means that the shear stress necessary to induce the melting of the phase is smaller when the system becomes softer. This result can be intuitively understood. In Ref. [20], we have argued that the elastic modulus $G_0$ measured on a macroscopic polycrystalline sample is the microscopic elastic constant of the hexagonal phase, which corresponds to a shear deformation of the triangular lattice [23]. Consequently, the modulus $G_0$ does not depend on the texture of the sample (i.e., the large scale polycrystalline arrangement) but is directly related to the interactions that maintain the 2D long-range order of the cylinders. The

smaller $G_0$, the weaker the interactions maintaining the 2D crystalline order and, therefore, the lower the stress necessary to overcome these interactions and thus, melt the system. However, despite its apparent simplicity, this result is not easy to be accounted for quantitatively. It would require a microscopic model to explain the origin of the shear melting, which is at present lacking. Such dependence on the elasticity of the material seems, nevertheless, general. For 3D colloidal crystals, Chen and Zukoski [5] found a critical stress for shear melting proportional to the shear modulus of the material. In the case of lamellar phases, dynamic transitions have also been found to occur at smaller critical stresses and rates when the systems become softer. Some tentative theoretical models exist in this case [24,25], which account for a dependence with the bulk modulus of the sample, but they are very specific, and *a priori* cannot be generalized to other types of dynamic transitions.

### B. Physical meanings of the transition temperature and activation energy

The analysis of the temperature dependence of the flow curves has evidenced the key role of the transition temperature $T_c$ and of the activation energy $E_A$. Let us comment briefly these two quantities.

#### *1. Transition temperature*

We have shown that all the quantities characterizing the flow curves vary critically with temperature and are equal to zero at the transition temperature $T_c = 12\,^\circ\mathrm{C}$ [Eq. (7)]. As determined by x-ray scattering, this temperature is precisely the transition temperature from the liquid crystalline phase to an isotropic liquid state. The temperature dependence of the flow curves proves naturally and expectedly that the shape of the flow curve and the numerical values of the rate-dependent stresses are intrinsic to the liquid crystalline order. Additional proof comes to the fact that, below $T_c$, the system presents a Newtonian behavior over a large range of shear rates and no dynamic transition is observed.

#### *2. Activation energy*

From the analysis of the variation of the flow curves with temperature, it appears that only one activation energy $E_A$ is involved. $E_A$ controls the shear thinning behavior at low shear rates, the shear-melting transition, and the Newtonian behavior at high shear rates. A unique activation energy seems, therefore, involved in the flow properties of, at the same time, a hexagonal phase with a 2D long-range order and a 2D liquid of cylinders. The energy $E_A$ cannot, therefore, be intrinsic to the crystalline order as it will be if related, for instance, to the density of dislocations. We propose $E_A$ to be related to the end-cap energy of the oil-swollen cylinders and to account for the energetic cost of cutting one cylinder into two pieces. The value of $E_A$ of 30 $kT$ is a correct order of magnitude [26], although all previous measurements for the scission energy of surfactant cylinders have been performed on pure surfactant systems and not on oil-swollen cylinders.

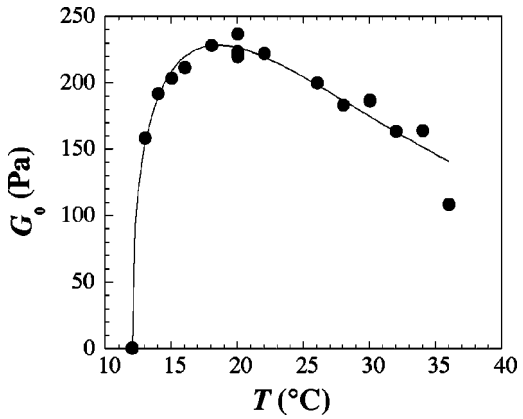


FIG. 10. Elastic modulus $G_0$ as a function of temperature for a sample with a swelling ratio $\rho = 3.24$. The line is a best fit of the data points (see text).

Based on this assertion, the nonmonotonous variation of the shear modulus $G_0$ with temperature can be qualitatively understood. Results are reported in Fig. 10 and show that $G_0$ is an increasing function of temperature at low $T$ and a decreasing function at high $T$. The elastic modulus is equal to zero at the transition temperature to an isotropic liquid phase, $T_c = 12\,^\circ\mathrm{C}$ and is maximal for $T$ around 20 °C. Although not theoretically justified, a test function of the form $(T - T_c)^p \times \exp(E/kT)$ (with $E = 17.5\ kT$ and $p = 0.4$) satisfactorily fits the experimental data (Fig. 10). It, moreover, provides a qualitative interpretation for the nonmonotonous variation of $G_0$ with $T$. On one hand, it indicates that the closeness to the isotropic transition dominates at low temperature and is responsible for the critical variation of $G_0$ with temperature. On the other hand, at high temperature, we propose the value of $G_0$ to be dominated by defects of end-cap type.

Indeed, the physics of vortex lattices is relevant to columnar liquid crystals and defects, such as vacancy and interstitial lines, exist in both types of systems [27]. As has been shown for vortex lines, the presence of these defects induces a decrease of the shear modulus of the system with a softening that depends exponentially on the density of defects [28]. In our system, we believe that the density of end caps is thermally activated with activation energy $E_A$. As temperature increases, the number of end caps is, therefore, expected to increase, which in turn, would lead to a decrease of the shear modulus $G_0$. This effect would be responsible for the decrease of $G_0$ with $T$ observed at high temperature ($T > 20\,^\circ\mathrm{C}$).

## V. CONCLUSION

We have investigated the behavior of soft lyotropic hexagonal phases under shear. By combining rheology and x-ray scattering under shear, we have recently shown that these systems present, above a critical stress and shear rate, a dynamic transition, which leads to a melting of the long-range two-dimensional order of the cylinders. In this paper, we have addressed the variation of the flow curve with two independent control parameters, temperature and swelling ratio

of the hexagonal phase. We have shown that a unified picture is emerging from the two series of experimental data. We have proven that the nonlinear rheology and, in particular, the shear-melting transition are solely controlled by the linear elasticity of the system. The shear elastic modulus $G_0$ of the hexagonal phase, which can be adjusted by varying either the swelling or the temperature, has indeed appeared as a key parameter. Moreover, in the particular case where temperature is varied, $G_0$ and the parameters characterizing the flow curves exhibit a nonmonotonous variation with temperature. We were able to interpret this nontrivial dependence as resulting from a combination of a thermally activated process, associated with the formation of end caps, and a critical variation with temperature, with a critical temperature equal to the transition temperature towards the liquid isotropic phase. Despite its valuable information, the detailed investigation presented in this paper is probably insufficient to unambiguously determine the physical mechanism for the shear melting. This certainly would require a theoretical approach, in particular, taking into account the very specific types of defect of columnar phases [27,29].

## ACKNOWLEDGMENTS

We thank F. Molino and G. Porte for fruitful discussions and L. Cipelletti for a critical reading of the manuscript.

[1] P.D. Olmsted and C.Y.D. Lu, Phys. Rev. E **56**, 55 (1997); P.D. Olmsted, Europhys. Lett. **48**, 339 (1999).
[2] V. Schmitt, C.M. Marques, and F. Lequeux, Phys. Rev. E **52**, 4009 (1995).
[3] G.A. McConnell, M.Y. Lin, and A.P. Gast, Macromolecules **28**, 6754 (1995).
[4] B.J. Ackerson and P.N. Pusey, Phys. Rev. Lett. **61**, 1033 (1988).
[5] L.B. Chen and C.F. Zukoski, Phys. Rev. Lett. **65**, 44 (1990).
[6] E. Eiser, F. Molino, G. Porte, and O. Diat, Phys. Rev. E **61**, 6759 (2000).
[7] O. Diat, D. Roux, and F. Nallet, J. Phys. III **3**, 1427 (1993); D. Roux, F. Nallet, and O. Diat, Europhys. Lett. **24**, 53 (1993).
[8] J. Yamamoto and H. Tanaka, Phys. Rev. Lett. **74**, 932 (1995).
[9] D. Bonn, J. Meunier, O. Greffier, A. Al-Kahwaji, and H. Kellay, Phys. Rev. E **58**, 2115 (1998).
[10] C. Meyer, S. Asnacios, C. Bourgaux, and M. Kleman, Mol. Cryst. Liq. Cryst. **332**, 531 (1999); C. Meyer, S. Asnacios, C. Bourgaux, and M. Kleman, Rheol. Acta **39**, 223 (2000).
[11] F.A. Morrison, J.W. Mays, M. Muthukumar, A.I. Natakani, and C.C. Han, Macromolecules **26**, 5271 (1993).
[12] T. Tepe, M.F. Schulz, J. Zhao, M. Tirrell, F.S. Bates, K. Mortensen, and K. Almdal, Macromolecules **28**, 3008 (1995), and references therein.
[13] W. Richtering, J. Läuger, and R. Linemann, Langmuir **10**, 4374 (1994); G. Schmidt, S. Müller, P. Lindner, C. Schmidt, and W. Richtering, J. Phys. Chem. B **102**, 507 (1998).
[14] L. Ramos and P. Fabre, Langmuir **13**, 682 (1997).
[15] L. Ramos, F. Molino, and G. Porte, Langmuir **16**, 5846 (2000).
[16] P. Ekwall, *Advances in Liquid Crystals*, edited by G. M. Brown (Academic Press, New York, 1975).
[17] L. Ramos (unpublished).
[18] A.-S. Wunenburger, A. Colin, J. Leng, A. Arnéodo, and D. Roux, Phys. Rev. Lett. **86**, 1374 (2001).
[19] Note that for $T=20\,°C$, $\tilde{\sigma}_p$ and $\Delta\tilde{\sigma}_p$ are by definition equal to $\sigma_p$ and $\Delta\sigma_p$. This is the case for the data obtained for different swelling ratios.
[20] L. Ramos and F. Molino, Europhys. Lett. **51**, 320 (2000).
[21] The elastic modulus is taken as being the storage modulus $G'$ obtained in the linear regime of oscillatory experiments at a frequency of 0.1 Hz performed on a polycrystalline sample. Note that this simple experimental determination gives quantitatively similar results as the measurements using creep tests [20], which validates the method used here.
[22] The cluster of points that clearly lies below the straight line corresponds to data taken at low temperature ($13\,°C \leqslant T \leqslant 16\,°C$), i.e., close to the transition temperature towards the isotropic phase. This suggests a physical reason at the origin of this discrepancy rather than experimental uncertainties, but it remains at present unclear.
[23] P.-G. de Gennes and J. Prost, *The Physics of Liquid Crystals* (Clarendon, Oxford, 1993).
[24] A.G. Zilman and R. Granek, Eur. Phys. J. B **11**, 593 (1999).
[25] A.S. Wunenberger, A. Colin, T. Colin, and D. Roux, Eur. Phys. J. E **2**, 277 (2000).
[26] M.E. Cates and S.J. Candau, J. Phys.: Condens. Matter **2**, 6869 (1990); J. Narayanan, W. Urbach, D. Langevin, C. Manohar, and R. Zana, Phys. Rev. Lett. **81**, 228 (1998).
[27] S. Jain and D.R. Nelson, Phys. Rev. E **61**, 1599 (2000).
[28] H.M. Carruzzo and C.C. Yu, Philos. Mag. B **77**, 1001 (1998); Phys. Rev. B **61**, 1521 (2000).
[29] J. Prost, Liq. Cryst. **8**, 123 (1990).